

# Compatibility-based selection of native fungi from oil palm empty fruit bunches for potential consortium development

NURHAIDA WIDIANI<sup>1,2</sup>, BAMBANG IRAWAN<sup>3,\*</sup>, ROCHMAH AGUSTRINA<sup>3</sup>, ANDI SETIAWAN<sup>4</sup>

<sup>1</sup>Doctoral Program of Mathematics and Natural Sciences, Faculty of Mathematics and Natural Sciences, Universitas Lampung. Jl. Prof. Dr. Soemantri Brodjonegoro No. 1, Gedung Meneng, Bandar Lampung 35145, Lampung, Indonesia

<sup>2</sup>Department of Biology, Faculty of Science and Technology, Universitas Islam Negeri Raden Intan. Jl. Letkol Endro Suratmin, Sukarame, Bandar Lampung 35131, Lampung, Indonesia

<sup>3</sup>Department of Biology, Faculty of Mathematics and Natural Sciences, Universitas Lampung. Jl. Prof. Dr. Soemantri Brodjonegoro No. 1, Gedung Meneng, Bandar Lampung 35145, Lampung, Indonesia. Tel.: +62-721-704625, \*email: bambang.irawan@fmipa.unila.ac.id

<sup>4</sup>Department of Chemistry, Faculty of Mathematics and Natural Sciences, Universitas Lampung. Jl. Prof. Dr. Soemantri Brodjonegoro No. 1, Gedung Meneng, Bandar Lampung 35145, Lampung, Indonesia

Manuscript received: 20 April 2026. Revision accepted: 31 May 2026.

**Abstract.** *Widiani N, Irawan B, Agustina R, Setiawan A. 2026. Compatibility-based selection of native fungi from oil palm empty fruit bunches for potential consortium development. Asian J Agric 10 (1): g100169. <https://doi.org/10.13057/asianjagric/g100169>. Oil palm empty fruit bunches (EFB) are an abundant lignocellulosic biomass in tropical agroecosystems but remain underutilized due to their recalcitrant structure and slow natural decomposition. This study aimed to isolate native fungal strains from EFB and evaluate their compatibility as a basis for selecting candidates for microbial consortium development. Twelve fungal isolates were successfully obtained and morphologically characterized, predominantly belonging to the genus *Aspergillus*, with representatives of *Penicillium* and *Mucor*. Interactions among isolates were evaluated using a dual culture assay, revealing diverse compatibility patterns. Of the 50 pairings evaluated, 32% were classified as compatible, 24% as partially compatible, and 44% as incompatible, indicating that antagonistic interactions were prevalent among the isolates. To further investigate interaction dynamics, compatibility data were analyzed using Cooperativeness Scoring (CS), heatmap visualization, and network analysis. These approaches enabled a quantitative and structural assessment of interaction patterns, demonstrating that compatibility among isolates is selective rather than universal. Isolates such as BKR10, BKR2, and BKR3 showed relatively high compatibility and central positions within the interaction network, indicating their potential as candidates for consortium development based solely on compatibility metrics. However, it should be noted that this study was limited to in vitro interaction assays, and functional lignocellulose degradation was not evaluated. Therefore, the identified isolates should be regarded as preliminary candidates that require further functional validation. This study provides a systematic framework for compatibility-based selection of native fungal isolates associated with EFB.*

**Keywords:** Compatibility screening, dual culture assay, empty fruit bunch composting, fungal interaction network, lignocellulose biomass

## INTRODUCTION

The oil palm industry is one of the most important agro-industrial sectors in tropical regions, particularly in Indonesia, where it contributes significantly to economic growth and rural development. However, the rapid expansion of oil palm plantations has led to the generation of large quantities of solid waste, especially oil palm Empty Fruit Bunches (EFB). EFB is a lignocellulosic biomass composed mainly of cellulose, hemicellulose, and lignin, which makes it highly resistant to natural degradation (Castano et al. 2019; Tahir et al. 2019; Arryanto et al. 2020). Improper management of this waste can result in environmental issues, including greenhouse gas emissions, nutrient imbalance, and soil degradation (Ferronato and Torretta 2019; Supriatna et al. 2022). Therefore, sustainable strategies for EFB utilization are urgently needed.

Composting is widely recognized as an environmentally friendly approach for converting organic waste into valuable soil amendments. However, the efficiency of composting lignocellulosic materials such as EFB is often

limited by their complex structure and low biodegradability (Supriatna et al. 2022). The decomposition of lignocellulosic biomass largely depends on the activity of microorganisms, particularly fungi, which play a key role in breaking down complex polymers through the secretion of extracellular enzymes such as cellulases, hemicellulases, and ligninases (Pérez-Contreras et al. 2025; Chen et al. 2025). Fungi associated with lignocellulosic substrates are therefore considered important agents in biomass conversion and nutrient cycling.

Previous studies have demonstrated that certain fungal genera, including *Aspergillus*, *Penicillium*, and *Mucor*, exhibit significant potential in degrading lignocellulosic materials under laboratory and field conditions (Matas-Baca et al. 2022). In addition, isolating fungi directly from natural substrates such as EFB is an important strategy for obtaining indigenous strains that are already adapted to local environmental conditions and substrate characteristics (Yu et al. 2023). Such native isolates are often better adapted to site-specific conditions compared to introduced strains.

To enhance decomposition efficiency, the use of microbial consortia has been increasingly explored. Unlike single isolates, microbial consortia can exhibit synergistic interactions that improve substrate colonization, enzyme production, and overall degradation performance (Irawan et al. 2019; Cui et al. 2021). However, the success of such consortia depends not only on the functional capabilities of individual members but also on their interaction dynamics. Microbial interactions can be cooperative, neutral, or antagonistic, and these interactions play a critical role in determining the stability and effectiveness of the consortium (de Boer 2017). In particular, antagonistic interactions, often mediated by competition for resources or the production of inhibitory metabolites, may suppress the growth of certain members and reduce overall system performance (Boddy 2000).

Compatibility assessment represents a critical preliminary step in consortium design, as microbial interactions determine whether coexisting isolates can establish stable communities. Even when individual isolates possess degradative potential, antagonistic interactions may inhibit growth and limit cooperative behavior. Therefore, evaluating compatibility prior to functional screening is essential to identify isolates that can coexist without inhibitory effects.

Despite growing interest in microbial consortia for lignocellulosic biomass conversion, most studies have focused primarily on enzymatic activity or degradation efficiency of individual isolates. Systematic evaluation of compatibility among indigenous fungal isolates, especially those derived from EFB, remains limited. Moreover, integrative approaches that combine compatibility assessment with quantitative and network-based analyses are still rarely applied in the context of consortium design, particularly in tropical agroecosystems.

Although lignocellulose degradation is a key functional trait, this study focuses on inter-isolate compatibility as an initial screening step. Functional evaluation, including enzymatic activity and degradation performance, was beyond the scope of this study and is proposed for future investigation. This study emphasizes systematic compatibility mapping among native EFB-derived fungi and integrates cooperativeness scoring with network-based analysis to provide a quantitative framework for evaluating interaction patterns.

In this context, exploring native fungal communities from EFB collected at PTPN VII Unit Bekri, Lampung, Indonesia, provides an opportunity to identify locally adapted isolates and evaluate their interaction patterns. Understanding these interactions is important for identifying isolates that can coexist and potentially function together in a microbial consortium.

Based on these considerations, this study aimed to isolate native fungal strains from EFB and evaluate their inter-isolate compatibility using dual culture assays combined with quantitative and network-based analyses. This study addresses the following research question: Do native fungal isolates from EFB exhibit interaction patterns that support their selection for consortium development? It is hypothesized that only a subset of isolates will exhibit

compatible interactions, reflecting the selective nature of microbial coexistence in lignocellulosic environments, consistent with ecological coexistence theory, which emphasizes the role of microbial interactions in structuring stable communities.

## MATERIAL AND METHODS

### Fungal isolation

Fungal isolates were obtained from oil palm Empty Fruit Bunches (EFB) collected in December 2022 from the oil palm processing residues at PT Perkebunan Nusantara VII, Bekri Unit, Lampung, Indonesia. Samples representing fresh, aged, and intermediate physical conditions were collected under field conditions and classified on observable characteristics, including color, texture, and degree of fiber degradation, rather than predetermined decomposition stages. The samples were transported to the laboratory in sterile plastic bags and stored at room temperature ( $28\pm 2^\circ\text{C}$ ) for 48 h prior to isolation. In this study, "native" fungi refer to isolates directly obtained from EFB at the collection site without prior enrichment or selective treatment, thereby minimizing bias in community composition. Fresh EFB was characterized by a light brown color, firm structure, and intact fibers, whereas intermediate EFB showed partial discoloration, moderate softening, and initial fiber breakdown. Aged EFB exhibited a dark brown to black color, soft texture, and advanced fiber decomposition. These categories were used to represent different stages of natural decomposition and to capture variability in fungal communities.

The isolation procedure followed the approach described by Irawan et al. (2022), which combines direct isolation with the moist chamber technique. EFB samples were aseptically cut into approximately 2 cm segments and surface-sterilized by sequential immersion in sterile distilled water (30s), 1% sodium hypochlorite (NaOCl) (1 min), and sterile distilled water (30s), followed by drying on sterile tissue paper.

Approximately 5-10 segments were placed in sterile Petri dishes lined with moistened filter paper to maintain a humid environment. The plates were incubated at room temperature ( $28\pm 2^\circ\text{C}$ ), and fungal growth emerging directly from the EFB segments was monitored daily for up to 30 days.

Emerging colonies were aseptically transferred onto Potato Dextrose Agar (PDA; Himedia, India) to obtain pure cultures. All procedures were conducted under aseptic conditions to minimize contamination. Isolation was continued throughout the incubation period until no additional morphologically distinct colonies were observed, indicating that the recovery of fungal isolates had reached a saturation point under the given experimental conditions. The resulting isolates were maintained on PDA slants at  $4^\circ\text{C}$  for subsequent analyses.

### Morphological characterization

Macroscopic characteristics, including colony color, texture, and growth pattern, were recorded after 7 days of

incubation on Potato Dextrose Agar (PDA). Microscopic observations were performed using lactophenol cotton blue staining and examined under a compound light microscope (Nikon 119c, Japan) at 400× magnification.

Diagnostic features, including hyphal septation, conidiophore structure, vesicle morphology, and conidial arrangement, were observed and used for identification. Fungal isolates were identified at the genus level only based on standard taxonomic keys (Barnett and Hunter 1998).

This morphology-based identification approach has inherent limitations, as morphological characteristics alone may not provide sufficient resolution for accurate species-level identification. Therefore, identification in this study was limited to the genus level. Molecular identification was not conducted and is recommended for future studies to improve taxonomic resolution and accuracy.

### Compatibility test

Compatibility among fungal isolates was evaluated using a dual culture technique following Mohammad et al. (2011). All possible pairwise combinations among isolates were tested under controlled laboratory conditions. The remaining combinations were excluded due to non-interpretable interactions, including inconsistent growth patterns or contamination that prevented reliable assessment. Pairings that resulted in non-interpretable interactions, such as contamination, inconsistent growth patterns, or unclear interaction boundaries, were excluded from further analysis.

For each pairing, mycelial plugs (5 mm in diameter) were taken from the actively growing margin of 7-day-old cultures and placed 4 cm apart on Potato Dextrose Agar (PDA) plates. The plates were incubated at 28±2°C for 7 days.

Colony interactions were visually assessed and classified into three categories based on predefined criteria: (i) Compatible, where colonies merged with hyphal intermingling and no visible inhibition zone; (ii) Partially compatible, where colonies made contact but maintained a distinct boundary without inhibition; and (iii) Incompatible, where a clear inhibition zone ( $\geq 2$  mm) or dominance/overgrowth of one isolate over the other was observed. Each pairing was performed in triplicate, and only interactions showing consistent patterns across replicates were included in the final analysis. Observations were conducted using standardized criteria to ensure consistency across replicates.

### Data analysis

Interaction outcomes from dual culture assays were expressed as percentages of total pairings and classified as Compatible (C), Partially Compatible (PC), or incompatible (I). To quantify compatibility at the isolate level, a Cooperativeness Score (CS) was calculated by assigning values of 1, 0.5, and 0 to C, PC, and I interactions, respectively. These weights were assigned to reflect a gradient of interaction strength, where fully compatible interactions contribute maximally to cooperativeness, partially compatible interactions represent

intermediate association, and incompatible interactions indicate absence of cooperative behavior. The cooperativeness score for each isolate ( $i$ ) was calculated as:

$$CS_i = \sum_{j=1}^{n_i} S_{ij}$$

Where,  $S_{ij}$  represents the interaction score between isolate  $i$  and isolate  $j$ , and  $n_i$  is the total number of valid pairings involving isolate  $i$ .

Compatibility patterns were visualized using a heatmap constructed from the interaction matrix. Network analysis was performed to identify relationships among isolates, where nodes represent fungal isolates and edges represent fully compatible interactions ( $C = 1$ ). Only fully compatible interactions were used to construct the network to emphasize stable and non-antagonistic associations among isolates. The network was treated as undirected, and degree centrality was used to identify highly connected (“hub”) isolates. Degree centrality was selected as a simple and interpretable metric to quantify the number of compatible connections for each isolate within the network.

All analyses were conducted using Python (version 3.10) with the following libraries: pandas (data handling), numpy (numerical analysis), matplotlib and seaborn (heatmap visualization), and networkx (network analysis). Default parameters were used unless otherwise specified.

## RESULTS AND DISCUSSION

### Morphological characterization of fungal isolates

Twelve fungal isolates (BKR1 - BKR12) were successfully obtained from oil palm Empty Fruit Bunches (EFB) collected at PTPN VII Unit Bekri, Lampung, Indonesia. Each isolate was subjected to macroscopic and microscopic morphological characterization to obtain preliminary taxonomic information (Table 1). Morphological observations revealed significant variations among isolates in terms of colony color, texture, and growth patterns. Representative macroscopic and microscopic features of the isolates are presented in Figure 1.

A comprehensive summary of macroscopic and microscopic characteristics used for preliminary identification is provided in Table 1. These characteristics serve as the basis for distinguishing among isolates and support the initial taxonomic classification at the genus level.

It should be noted that the present identification is based solely on morphological characteristics and may not provide sufficient resolution for accurate species level classification. Therefore, the assigned genera should be interpreted with caution, as closely related taxa may exhibit overlapping features. In addition, quantitative measurements of microscopic structures (e.g., conidiophore length or spore size) were not recorded in this study, which may limit the precision of morphological differentiation among isolates.

Although most isolates were assigned to the genus *Aspergillus*, this predominance should be interpreted carefully due to the limitations of morphology-based

identification and the potential for misclassification among morphologically similar genera.

The observed variation in colony morphology and microscopic structures highlights the diversity of fungal communities associated with EFB and provides a foundational basis for subsequent compatibility and interaction analyses. Based on these morphological characteristics, further analysis was conducted to evaluate inter-isolate interactions and compatibility using dual culture assays.

### Fungal compatibility evaluation

The dual culture assay was conducted to evaluate interaction patterns among fungal isolates obtained from EFB collected at PTPN VII, Bekri Unit, Indonesia. Interactions between fungal colonies were assessed based on inhibition zones, direct contact, and colony fusion, following the criteria described by Mohammad et al. (2011).

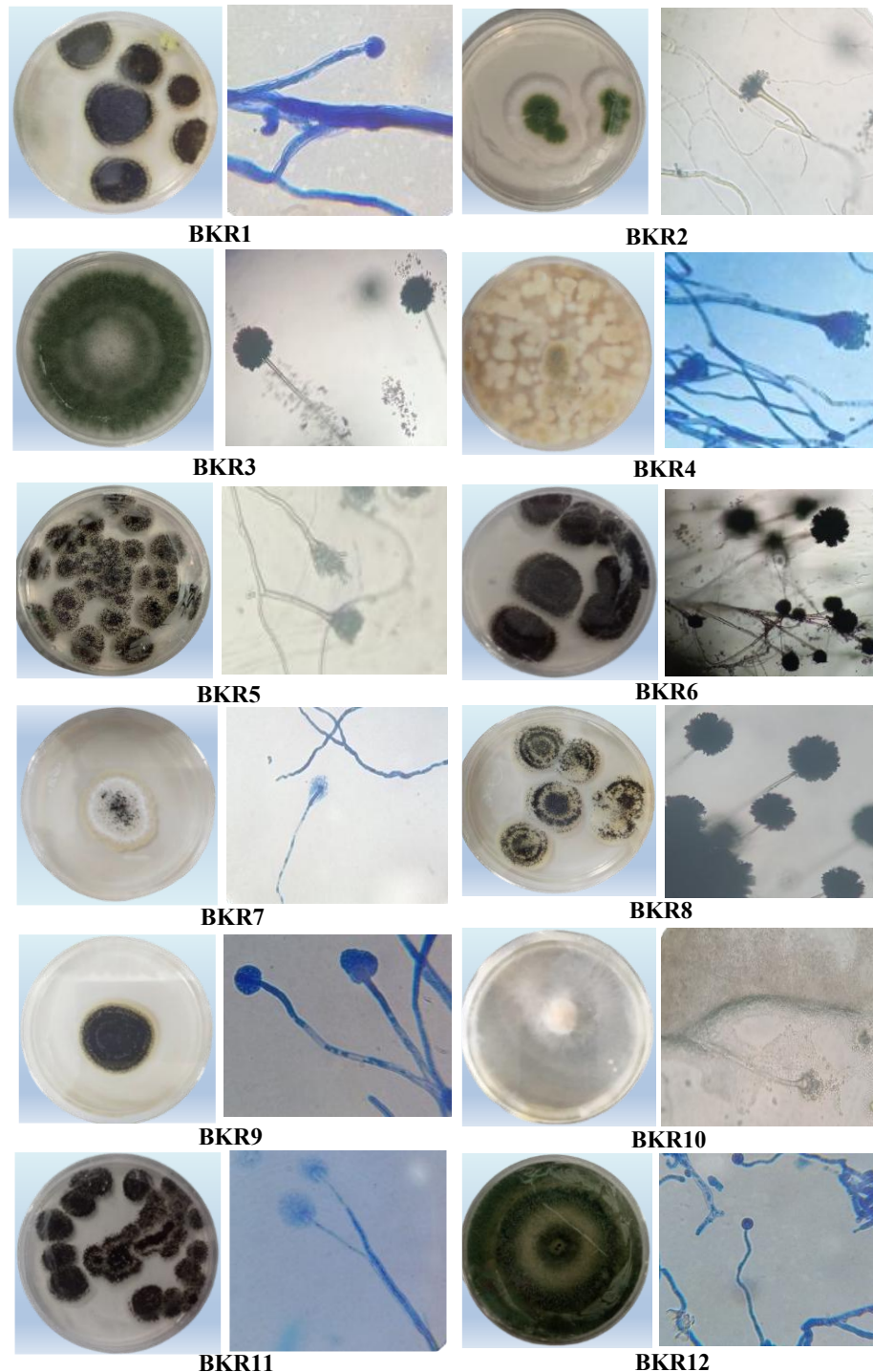


**Figure 1.** Macroscopic and microscopic morphology of fungal isolates grown on PDA after 7 days of incubation at 28±2°C

Of 50 isolate pairings tested, 32% (16 combinations) were classified as compatible, 24% (12 combinations) showed partially compatible, and 44% (22 combinations) as incompatible (Table 2). Although a total of 66 pairwise combinations were theoretically possible among the isolates, only 50 pairings were included in the final analysis. The remaining combinations were excluded due to non-interpretable outcomes, such as contamination, inconsistent growth patterns, or unclear interaction boundaries that prevented reliable classification. These exclusions were not associated with specific isolates but were distributed across different combinations.

Compatible interactions were identified by colony merging without visible inhibition zones, indicating mutual tolerance and hyphal integration (Figure 2). In these cases, the mycelia of both isolates grew toward each other and

fused at the point of contact, forming a continuous mycelial front without visible antagonism.

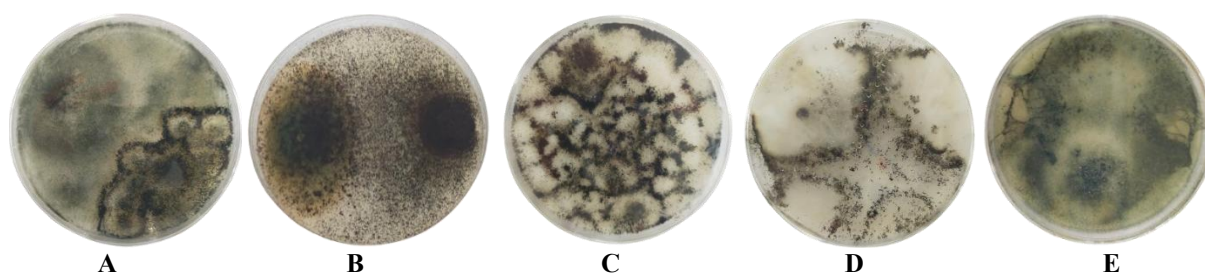
Partially compatible interactions occurred when colonies made contact but maintained a distinct boundary without clear inhibition (Figure 3). These interactions indicated limited integration between colonies while still allowing direct contact.

In contrast, incompatible interactions were characterized by the presence of inhibition zones, colony dominance, or restricted growth at the interaction interface (Figure 4). In some pairings, growth halted at the point of contact, forming a stable boundary between colonies. The relatively high proportion of incompatible interactions (44%) indicates that antagonistic interactions were frequently observed among the tested isolates.

**Table 1.** Macroscopic and microscopic identification of fungal isolates from oil palm empty fruit bunches

Isolate code	Macroscopic features	Microscopic features	Presumed genus
BKR1	Black colony with yellowish margins; velvety surface; radial growth with concentric zones	Septate hyphae; well-developed conidiophores terminating in vesicles; radiating phialides; dense globose conidia in chains	<i>Aspergillus</i> sp.
BKR2	White to green colony; smooth to velvety surface; circular growth with regular margins	Septate hyphae; upright conidiophores with vesicles; conidia arranged in moderately long chains	<i>Aspergillus</i> sp.
BKR3	Green colony with darker central zone; velvety texture; distinct radial pattern	Septate hyphae; conidiophores with vesicles; compact conidial heads with globose conidia	<i>Aspergillus</i> sp.
BKR4	Yellowish-brown colony; velvety surface; circular growth with clear radial pattern	Septate hyphae; elongated conidiophores ending in vesicles; radiating phialides; globose conidia	<i>Aspergillus</i> sp.
BKR5	Dark gray to black colony; powdery surface; rapid radial expansion	Septate hyphae; long conidiophores; loosely arranged globose conidia forming brush-like heads	<i>Aspergillus</i> sp.
BKR6	Black colony with darker margins; powdery texture; concentric radial growth	Septate hyphae; erect conidiophores; dense clusters of globose conidia forming compact heads	<i>Aspergillus</i> sp.
BKR7	White colony with dark speck formation; velvety surface; radial growth	Septate hyphae; relatively long conidiophores; conidia forming extended chains	<i>Aspergillus</i> sp.
BKR8	Dark colony with grayish margins; dense, powdery surface; circular growth	Septate hyphae; shorter conidiophores; globose conidia forming compact heads	<i>Aspergillus</i> sp.
BKR9	Dark colony with pale margins; velvety texture; radial growth pattern	Septate hyphae; conidiophores terminating in vesicles; radiating phialides; globose conidia in chains	<i>Aspergillus</i> sp.
BKR10	White to grayish colony; fluffy, cotton-like texture; rapid aerial growth; spreading colony	Non-septate (coenocytic) hyphae; sporangiophores bearing spherical sporangia; sporangiospores present	<i>Mucor</i> sp.
BKR11	White to dark gray colony; velvety surface; diffuse radial growth	Septate hyphae; conidiophores with vesicles; clustered globose conidia forming dense heads	<i>Aspergillus</i> sp.
BKR12	Green to bluish-green colony; velvety to powdery texture; circular growth with concentric zones	Septate hyphae; branched conidiophores forming penicillus-like structures; chains of conidia at tips	<i>Penicillium</i> sp.

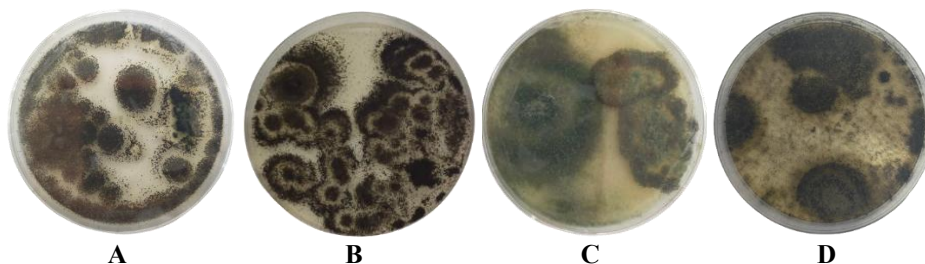
Note: Identification was based on morphological characteristics following Barnett and Hunter (1998) and limited to genus level



**Figure 2.** Compatible interaction between fungal isolates from EFB based on dual culture assay

**Table 2.** Classification of interactions among fungal isolates based on dual culture assay

Combination	Visual observation	Interaction type
BKR1 × BKR2	Colonies grow side by side with partial overlapping	Partially compatible
BKR1 × BKR3	Colonies do not merge, clear inhibition zone observed	Incompatible
BKR1 × BKR4	Colonies do not fully merge, thin inhibition zone present	Partially compatible
BKR1 × BKR5	Colonies clearly separated with distinct distance	Incompatible
BKR1 × BKR7	Colonies do not fully merge, thin inhibition zone present	Partially compatible
BKR1 × BKR8	Colonies merge completely without barriers	Compatible
BKR1 × BKR9	Colonies separated clearly, inhibition zone/antagonism/deadlock observed	Incompatible
BKR1 × BKR11	Colonies grow side by side with partial overlapping	Partially compatible
BKR1 × BKR12	Colonies grow side by side with thin inhibition zone	Partially compatible
BKR2 × BKR6	Colonies tend to merge without clear inhibition zone	Compatible
BKR2 × BKR8	Two colonies meet without clear inhibition zone	Compatible
BKR2 × BKR10	Colonies spread and meet	Compatible
BKR2 × BKR11	Colonies grow side by side with partial overlapping	Partially compatible
BKR2 × BKR12	Colonies do not merge, inhibition zone present	Incompatible
BKR3 × BKR4	Colonies grow merged	Compatible
BKR3 × BKR6	Colonies merge, no antagonism zone present	Compatible
BKR3 × BKR7	Colonies nearly merge with indistinct boundary	Compatible
BKR3 × BKR8	Dominance of one colony	Incompatible
BKR3 × BKR9	Colonies clearly separated, inhibition zone observed	Incompatible
BKR4 × BKR5	Colonies grow side by side without inhibition	Compatible
BKR4 × BKR6	Colonies do not merge, inhibition zone present	Incompatible
BKR4 × BKR7	Colonies grow side by side with partial overlapping	Partially compatible
BKR4 × BKR8	Partially merge with unclear contact zone	Partially compatible
BKR4 × BKR9	Colonies contact without inhibition zone	Compatible
BKR4 × BKR10	Partially merged growth with indistinct boundary	Partially compatible
BKR4 × BKR12	Colonies do not merge, inhibition zone present with BKR12 dominance	Incompatible
BKR5 × BKR6	Colonies fully merge, sporulation evenly distributed without clear boundary	Compatible
BKR5 × BKR8	Colonies do not merge, inhibition zone present	Incompatible
BKR5 × BKR9	Colonies do not merge, inhibition zone present	Incompatible
BKR5 × BKR10	Colonies meet and merge without clear separation, no inhibition zone observed	Compatible
BKR5 × BKR11	Clear inhibition zone between colonies, sharp boundary, no merging	Incompatible
BKR5 × BKR12	Colonies contact but do not merge	Partially compatible
BKR6 × BKR7	Colonies partially contact	Partially compatible
BKR6 × BKR8	Colonies clearly separated with inhibition zone/antagonism/deadlock	Incompatible
BKR6 × BKR10	Colonies grow merged with balanced sporulation	Compatible
BKR6 × BKR11	Clear inhibition zone, colonies do not merge	Incompatible
BKR6 × BKR12	Clear colony boundaries observed	Incompatible
BKR7 × BKR8	Clear inhibition zone, restricted growth	Incompatible
BKR7 × BKR9	Colonies partially contact	Partially compatible
BKR7 × BKR10	Colonies grow merged	Compatible
BKR7 × BKR11	Clear contact boundary, colonies do not merge	Incompatible
BKR7 × BKR12	Dominance of one colony	Incompatible
BKR8 × BKR9	Clear inhibition zone with mutual suppression	Incompatible
BKR8 × BKR10	Colonies merge and spread evenly	Compatible
BKR8 × BKR11	Colonies spread evenly	Compatible
BKR8 × BKR12	Dominance of one isolate with clear inhibition zone	Incompatible
BKR9 × BKR11	Clear contact boundary, colonies do not merge	Incompatible
BKR9 × BKR12	Dominance of one colony	Incompatible
BKR10 × BKR12	Even growth without mutual inhibition	Compatible
BKR11 × BKR12	Clear inhibition zone with one colony dominance	Incompatible

**Figure 3.** Partially compatible interaction between fungal isolates from EFB based on dual culture assay

Although inhibition zone widths were not quantitatively measured in this study, incompatible interactions were consistently identified based on clearly visible separation zones and growth suppression at the colony interface, in accordance with the predefined classification criteria. The consistency of interaction patterns across replicate assays supports the reliability of the visual classification approach.

Overall, the observed interaction patterns demonstrate substantial variability in compatibility among isolates. These results provide a basis for subsequent quantitative analyses, including cooperativeness scoring and network-based evaluation of interaction relationships among fungal isolates.

### Compatibility pattern analysis and network structure

Compatibility data were further analyzed using Cooperativeness Scoring (CS), heatmap visualization, and network analysis. A quantitative summary of interaction outcomes is presented in Table 3. The results showed that isolate BKR10 exhibited the highest cooperativeness score (CS = 0.92), followed by BKR2 (CS = 0.70) and BKR3 (CS = 0.60). In contrast, isolates such as BKR9 (CS = 0.08) and BKR12 (CS = 0.29) showed low compatibility, indicating a predominance of incompatible interactions.

The Cooperativeness Score (CS) provides a semi-quantitative ranking of isolates based on interaction outcomes using a weighted scoring scheme (1, 0.5, 0), reflecting a gradient of compatibility. Although no formal statistical sensitivity analysis was conducted, the consistency between CS values and observed interaction patterns supports the robustness of this approach.

The distribution of interaction patterns is further illustrated in Figure 5. Heatmap analysis (Figure 5.B) revealed heterogeneous compatibility patterns among isolates, confirming that interactions were selective rather than uniform across pairings, whereas network analysis (Figure 5.C) highlighted differences in connectivity.

Network analysis further quantified these differences by measuring the number of compatible connections (degree) for each isolate. BKR10 exhibited the highest connectivity ( $n = 5$ ), followed by BKR2, BKR3, and BKR8 ( $n = 3$  each). Isolates BKR4, BKR5, and BKR6 showed moderate connectivity ( $n = 2$ ), whereas BKR1, BKR7, BKR11, and BKR12 each formed only one compatible connection ( $n = 1$ ). Notably, BKR9 did not exhibit any compatible interactions ( $n = 0$ ), indicating minimal integration within the network.

These results provide a quantitative and visual representation of compatibility relationships among isolates. The agreement between cooperativeness scores and network connectivity further supports the reliability of the observed compatibility patterns. The integration of cooperativeness scoring with heatmap and network visualization enables clearer identification of interaction patterns across isolate pairings. Together, these analyses form the basis for further interpretation of interaction dynamics.

**Table 3.** Interaction outcomes and Cooperativeness Score (CS) of fungal isolates

Isolate	Compatible	Partially compatible	Incompatible	Total	CS
BKR1	1	5	3	9	0.39
BKR2	3	1	1	5	0.70
BKR3	3	0	2	5	0.60
BKR4	2	3	2	7	0.50
BKR5	2	1	3	6	0.42
BKR6	2	1	3	6	0.42
BKR7	1	2	3	6	0.33
BKR8	3	0	4	7	0.43
BKR9	0	1	5	6	0.08
BKR10	5	1	0	6	0.92
BKR11	1	1	4	6	0.25
BKR12	1	2	4	7	0.29

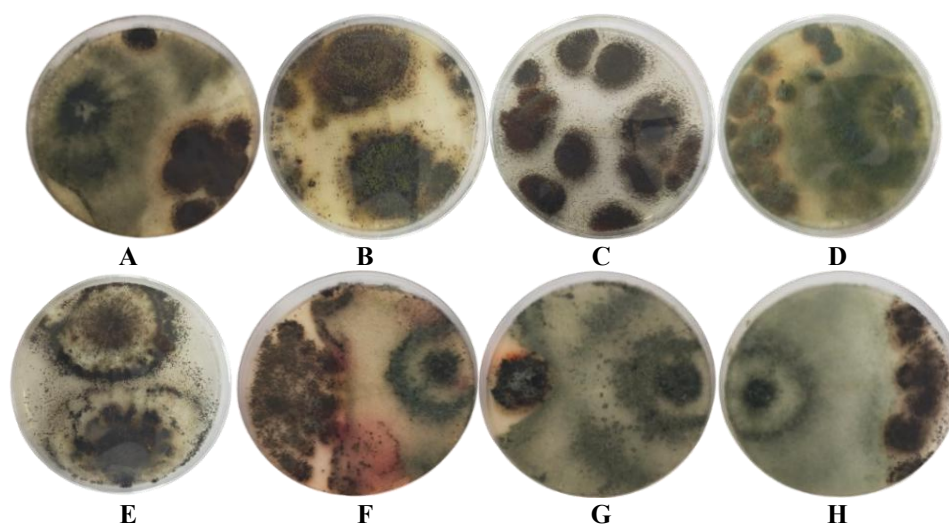


**Figure 4.** Incompatible interaction between fungal isolates from EFB based on dual culture assay

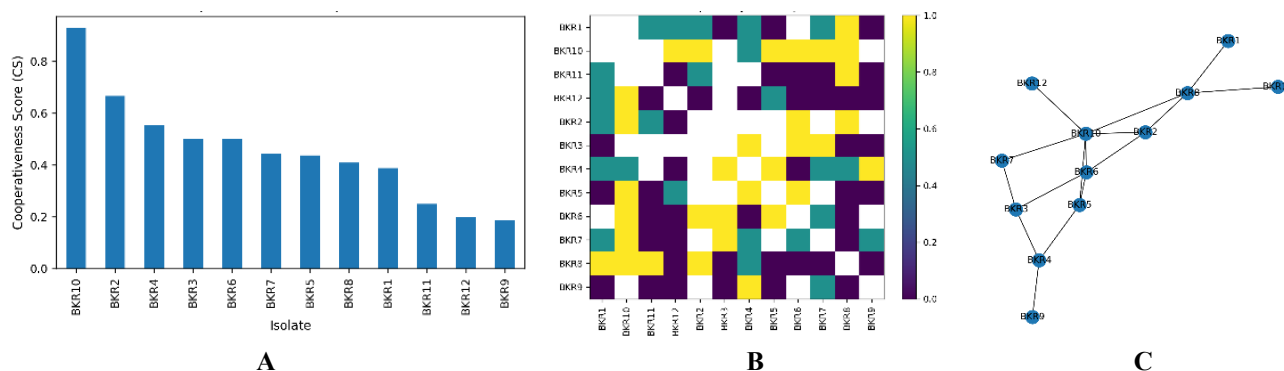


**Figure 5.** Compatibility analysis of fungal isolates. A. Cooperativeness Score (CS) indicating the compatibility potential of each isolate, B. Heatmap showing pairwise interaction patterns based on dual culture assays (1: Compatible; 0.5: Partially compatible; 0: Incompatible), C. Network diagram illustrating fully compatible interactions among isolates; where nodes represent isolates and edges indicate compatible pairings

## Discussion

This study provides a comprehensive evaluation of morphological diversity and interaction patterns among lignocellulolytic fungi isolated from oil palm Empty Fruit Bunches (EFB), highlighting their potential ecological relevance while acknowledging that functional implications for consortium performance were not directly evaluated in this study.

Morphological observations indicated that several isolates exhibited characteristics consistent with the genus *Aspergillus*, including dark-colored colonies with velvety to powdery textures, while BKR12 displayed features typical of *Penicillium*, and BKR10 corresponded to *Mucor*. These identifications were further supported by microscopic observations, where most isolates exhibited septate hyphae and conidiophore structures characteristic of *Aspergillus*, whereas BKR12 and BKR10 showed morphological traits consistent with *Penicillium* and *Mucor*, respectively. However, these identifications are based solely on morphological characteristics and should be interpreted with caution due to potential taxonomic uncertainty.

The occurrence of these genera is consistent with previous reports indicating that *Aspergillus*, *Penicillium*, and *Mucor* are commonly associated with lignocellulosic substrates and are known to contribute to biomass degradation through enzyme production (Andlar et al. 2018; Christopher et al. 2022; Pérez-Contreras et al. 2025). The lignocellulose degradation potential discussed in this study is inferred from genus-level identification and literature reports, and was not experimentally measured. Enzymatic activity was not measured in the present study, and therefore these functional roles are inferred from the literature rather than directly demonstrated. The predominance of *Aspergillus* is also in agreement with earlier studies highlighting its adaptability and enzymatic versatility (Salihu et al. 2015). In addition, *Penicillium* species are known for their ability to interact synergistically with other microorganisms, particularly under nutrient-limited or acidic conditions (Irawan et al. 2022; Pan et al. 2024), whereas *Mucor* species have been

reported to produce ligninolytic enzymes that contribute to lignin decomposition (Geethanjali et al. 2020).

The observed morphological diversity suggests that EFB serves as a suitable ecological niche for a broad range of saprophytic fungi. Although morphological characterization provides a useful basis for preliminary identification at the genus level, it remains insufficient for reliable species-level classification due to overlapping phenotypic traits. Therefore, molecular approaches, such as sequencing of the Internal Transcribed Spacer (ITS) region or protein-coding genes, are recommended for future studies to improve taxonomic resolution.

The dual culture assay revealed that antagonistic interactions were predominant (44%), followed by compatible (32%) and partially compatible interactions (24%). This dominance of antagonistic interactions indicates that coexistence among lignocellulolytic fungi is selective and influenced by ecological competition. Incompatible interactions, characterized by inhibition zones and growth restriction, are consistent with competitive mechanisms such as resource competition or the production of inhibitory metabolites reported in previous studies (Boddy 2000; de Boer 2017). Such patterns are consistent with previous findings indicating that microbial competition plays a central role in shaping community structure in lignocellulosic environments (Rastogi et al. 2020; Matas-Baca et al. 2022). While antagonistic interactions are often viewed as limiting factors, they may also contribute to community stability by regulating dominance and maintaining species balance under certain conditions.

Despite the predominance of antagonism, a subset of isolates exhibited relatively high compatibility. The relatively lower proportion of compatible interactions (32%) suggests that only a limited number of isolate combinations are suitable for stable coexistence. Compatible interactions may indicate mutual tolerance, whereas partially compatible reflects limited interaction that may still allow coexistence under certain conditions. Previous studies have reported that partially compatible

strains can still contribute to biodegradation processes, although with varying efficiency (Mohammad et al. 2011).

Further quantitative analysis using Cooperativeness Scoring (CS), heatmap visualization, and network analysis provided deeper insights into interaction patterns. The results showed that BKR10 exhibited the highest CS value and connectivity (degree = 5), followed by BKR2 and BKR3 (degree = 3), indicating their relatively central positions within the interaction network. These findings suggest that these isolates have higher compatibility potential based on interaction patterns, rather than confirming functional superiority. Such isolates may act as “hub isolates” within the network structure. Network-based approaches have been widely applied to identify key taxa and interaction hubs in microbial communities (Amit and Bashan 2023). The network topology in this study is based solely on compatibility interactions under *in vitro* conditions and does not necessarily reflect ecological interactions under natural or composting environments.

Conversely, isolates such as BKR9 and BKR12 exhibited low compatibility and limited connectivity, indicating a predominance of antagonistic behavior. This observation is consistent with their low cooperativeness score (CS = 0.08 and 0.29, respectively), which reflect a predominance of incompatible interactions. These isolates may be less suitable for co-culture systems due to their potential to inhibit the growth of other microorganisms, as previously reported in fungal interaction studies (Boddy 2000; de Boer 2017).

From an ecological perspective, the observed interaction patterns indicate that fungal communities in lignocellulosic environments are structured by both cooperative and competitive interactions. The high proportion of antagonistic interaction (44%) compared to compatible interactions (32%) further emphasizes the dominance of competitive dynamics in these communities. However, compatibility alone does not guarantee functional synergy in consortium performance. Functional traits such as enzyme production were not evaluated in this study, which limits direct inference regarding biodegradation efficiency. This is particularly relevant in lignocellulose decomposition, which depends on the coordinated activity of complex microbial communities (Osono 2020).

It is important to note that the interaction patterns observed in this study are based on *in vitro* dual culture assays conducted on PDA, which may not fully represent fungal interactions under natural composting conditions. Environmental complexity, substrate heterogeneity, and interactions with other microorganisms may influence compatibility dynamics differently. Therefore, the applicability of these results to field-scale or composting systems should be interpreted with caution, and further validation under more complex conditions is required.

The findings highlight the importance of compatibility-based screening as a preliminary step in microbial consortium development. Further validation through functional assays, such as enzymatic activity analysis and composting trials, is necessary before confirming the suitability of selected isolates for applied use.

This study demonstrates that compatibility among fungi is an important consideration in consortium design. The integration of morphological characterization, interaction assays, and quantitative analyses provides a framework for preliminary selection of isolates based on compatibility, rather than definitive functional performance.

In conclusion, this study successfully isolated and characterized twelve native fungal isolates from EFB, with preliminary identification indicating dominance of *Aspergillus* alongside *Penicillium* and *Mucor*. Compatibility assessment revealed diverse interaction patterns, with antagonistic interactions predominating and only a subset of isolates showing consistent compatibility, indicating that coexistence among fungal isolates is selective rather than universal. The integration of compatibility evaluation with cooperativeness scoring, heatmap visualization, and network analysis facilitated the identification of isolates with relatively high compatibility based on interaction metrics, particularly BKR10, BKR2, and BKR3, which occupied central positions within the interaction network. These isolates should be regarded as potential candidates for consortium development based solely on compatibility assessment, rather than confirmed functional decomposers. These findings highlight that compatibility-based selection is essential, as random combinations of isolates may lead to antagonistic interactions and reduced system stability. Compatibility alone does not guarantee functional synergy or degradation performance. Further studies incorporating molecular identification, enzymatic profiling, and functional validation are required to confirm the performance of selected isolates under applied conditions. This study provides a systematic framework for the rational selection of compatible fungal isolates associated with lignocellulosic biomass for potential application in biomass management within tropical agroecosystems.

## ACKNOWLEDGEMENTS

The authors gratefully acknowledge the support of PT Perkebunan Nusantara VII, Bekri Unit, Lampung, Indonesia, for providing access to the oil palm Empty Fruit Bunches (EFB) samples. We also extend our sincere thanks to the Laboratory of Microbiology, Universitas Lampung and Laboratory of UIN Raden Intan Lampung for providing laboratory facilities and technical support throughout the study. This research did not receive any specific grant from funding agencies in the public, commercial, or not-for-profit sectors. The authors declare that there are no conflicts of interest regarding the publication of this paper.

## REFERENCES

- Amit G, Bashan A. 2023. Top-down identification of keystone taxa in the microbiome. *Nat Commun* 14 (1): 3951. <https://doi.org/10.1038/s41467-023-39459-5>.
- Andlar M, Rezić T, Mardetko N, Kracher D, Ludwig R, Šantek B. 2018. Lignocellulose degradation: An overview of fungi and fungal

- enzymes involved in lignocellulose degradation. *Eng Life Sci* 18 (11): 768-778. <https://doi.org/10.1002/elsc.201800039>.
- Arryanto D, Nasution Z, Rauf A. 2020. Dynamics of K, Ca, Mg in spodosol land that is applied oil palm empty fruit bunch on oil palm cultivation land (*Elaeis guineensis* Jacq.) in Central Kalimantan. IC2RSE 2019. <https://doi.org/10.4108/eai.4-12-2019.2293832>.
- Barnett H. Hunter BB. 1998. *Illustrated Genera of Imperfect Fungi*. 4<sup>th</sup> Edition. APS Press, St. Paul.
- Boddy L. 2000. Interspecific combative interactions between wood-decaying basidiomycetes. *FEMS Microbiol Ecol* 31 (3): 185-194. [https://doi.org/10.1016/S0168-6496\(99\)00093-8](https://doi.org/10.1016/S0168-6496(99)00093-8).
- Castano JD, Crespo CC, Torres E. 2019. Evaluation of chemical and biological treatments to degrade oil palm empty fruit bunches (*Elaeis guineensis* Jacq.) and their potential use. *J Oil Palm Res* 31 (2): 271-280. <https://doi.org/10.21894/jopr.2019.0016>.
- Chen M, Li Q, Liu C, Meng E, Zhang B. 2025. Microbial degradation of lignocellulose for sustainable applications. *Sustainability* 17 (9): 4223. <https://doi.org/10.3390/su17094223>.
- Christopher M, Sreeja-Raju A, Sankar M, Gokhale DV, Pandey A, Sukumaran RK. 2022. Lignocellulose degradation by *Penicillium janthinellum* enzymes is influenced by its variable secretome and a unique set of feedstock characteristics. *Bioresour Technol* 365: 128-129. <https://doi.org/10.1016/j.biortech.2022.128129>.
- Cui T, Yuan B, Guo H, Tian H, Wang W, Ma, Y, Li C, Fei, Q. 2021. Enhanced lignin biodegradation by consortium of white rot fungi: Microbial synergistic effects and product mapping. *Biotechnol Biofuels* 14 (1): 162. <https://doi.org/10.1186/s13068-021-02011-y>.
- de Boer W. 2017. Upscaling of fungal-bacterial interactions: From the lab to the field. *Curr Opin Microbiol* 37: 35-41. <https://doi.org/10.1016/j.mib.2017.03.007>.
- Ferronato N, Torretta V. 2019. Waste mismanagement in developing countries: A review of global issues. *Intl J Environ Res Public Health* 16 (6): 1060. <https://doi.org/10.3390/ijerph16061060>.
- Geethanjali PA, Gowtham HG, Jayashankar M. 2020. Biodegradation potential of indigenous litter dwelling ligninolytic fungi on agricultural wastes. *Bull Natl Res Cent* 44 (1): 173. <https://doi.org/10.1186/s42269-020-00426-5>.
- Irawan B, Kasiandari RS, Sunarminto BH, Soetarto ES, Hadi S. 2019. Effect of fungal inoculum application on changes in organic matter of leaf litter composting. *Pol J Soil Sci* 52 (1): 143-152. <https://doi.org/10.17951/pjss/2019.52.1.143>.
- Irawan B, Wahyuningtias, I, Ayuningtyas N, Isky OA, Farisi S, Sumardi S, Afandi A, Hadi S. 2022. Potential lignocellulolytic microfungi from pineapple plantation for composting inoculum additive. *Intl J Microbiol* 2022: 9252901. <https://doi.org/10.1155/2022/9252901>.
- Matas-Baca MÁ, Urias García C, Pérez-Álvarez S, Flores-Córdova MA, Escobedo-Bonilla CM, Magallanes-Tapia MA, Sánchez Chávez, E. 2022. Morphological and molecular characterization of a new autochthonous *Trichoderma* sp. isolate and its biocontrol efficacy against *Alternaria* sp. *Saudi J Biol Sci* 29 (4): 2620-2625. <https://doi.org/10.1016/j.sjbs.2021.12.052>.
- Mohammad N, Alam MZ, Kabashi NA, Adebayo OS. 2011. Development of compatible fungal mixed culture for composting process of oil palm industrial waste. *Afr J Biotechnol* 10 (81): 18657-18665. <https://doi.org/10.5897/AJB11.2735>.
- Osono T. 2020. Functional diversity of ligninolytic fungi associated with leaf litter decomposition. *Ecol Res* 35 (1): 30-43. <https://doi.org/10.1111/1440-1703.12063>.
- Pan C, Sun C, Qu X, Yu W, Guo J, Yu Y, Li X. 2024. Microbial community interactions determine the mineralization of soil organic phosphorus in subtropical forest ecosystems. *Microbiol Spectr* 12 (3): e0135523. <https://doi.org/10.1128/spectrum.01355-23>.
- Pérez-Contreras, S, Avalos-de la Cruz DA, Lizardi-Jiménez MA, Herrera-Corredor JA, Baltazar-Bernal O, Hernández-Martínez R. 2025. Production of ligninolytic and cellulolytic fungal enzymes for agro-industrial waste valorization: Trends and applicability. *Catalysts* 15 (1): 30. <https://doi.org/10.3390/catal15010030>.
- Rastogi M, Nandal M, Khosla B. 2020. Microbes as vital additives for solid waste composting. *Heliyon* 6 (2): e03343. <https://doi.org/10.1016/j.heliyon.2020.e03343>.
- Salihu A, Abbas O, Sallau AB, Alam MZ. 2015. Agricultural residues for cellulolytic enzyme production by *Aspergillus niger*: Effects of pretreatment. *3 Biotech* 5 (6): 1101-1106. <https://doi.org/10.1007/s13205-015-0294-5>.
- Supriatna J, Setiawati MR, Sudirja R, Suherman C, Bonneau X. 2022. Composting for a more sustainable palm oil waste management: A systematic literature review. *Sci World J* 2022: 5073059. <https://doi.org/10.1155/2022/5073059>.
- Tahir PM, Liew WPP, Lee SY, Ang, AF, Lee SH, Mohamed R, Halis R. 2019. Diversity and characterization of lignocellulolytic fungi isolated from oil palm empty fruit bunch, and identification of influencing factors of natural composting process. *Waste Manag* 100: 128-137. <https://doi.org/10.1016/j.wasman.2019.09.002>.
- Yu J, Lai J, Neal BM, White BJ, Banik MT, Dai SY. 2023. Genomic diversity and phenotypic variation in fungal decomposers involved in bioremediation of persistent organic pollutants. *J Fungi* 9 (4): 418. <https://doi.org/10.3390/jof9040418>.